Cell Research (2012) 22:259-272.

www.nature.com/cr

ORIGINAL ARTICLE

The critical role of $CD133^{+}CD44^{+/high}$ tumor cells in hematogenous metastasis of liver cancers

Ying Hou[1, 2, *], Qifei Zou[3, *], Ruiliang Ge[3], Feng Shen[3], Yizheng Wang[1]

[1]State Key Laboratory of Neuroscience, Institute of Neuroscience, Shanghai Institutes for Biological Sciences, 320 Yueyang Road, Shanghai 200031, China; [2]Graduate School, The Chinese Academy of Sciences; [3]Eastern Hepatobiliary Surgery Hospital, Second Military Medical University, 225 Changhai Road, Shanghai 200438, China

Metastatic hepatocellular carcinoma (HCC) is one of the most lethal cancers worldwide. However, the cell population responsible for its metastasis remains largely unknown. Here, we reported that $CD133^{+}CD44^{+/high}$ defined a subgroup of tumor cells that was responsible for hematogenous metastasis of liver cancers. Immunohistochemical investigation of human HCC specimens revealed that the number of $CD133^{+}$ and $CD44^{+}$ HCC cells was increased and was associated with portal vein invasion. Purified $CD133^{+}$ or $CD44^{high}$ HCC cells were superior in clonogenic growth and vascular invasion, respectively. Thus, the combination of CD133 and CD44 was used to define a novel HCC subpopulation. $CD133^{+}CD44^{high}$, but not $CD133^{+}CD44^{low/-}$, $CD133^{-}CD44^{high}$ or $CD133^{-}CD44^{low/-}$ xenografts, produced intrahepatic or lung metastasis in nude mice. Further analysis of human HCC samples by flow cytometry showed that the number of $CD133^{+}CD44^{+}$ tumor cells was associated with portal vein metastasis. The cDNA microarray analysis of $CD133^{+}CD44^{+}$ and $CD133^{+}CD44^{-}$ tumor cells isolated from metastatic HCC patients revealed that these cells comprised of two different populations possessing distinct gene expression profiles. Our results suggest that $CD133^{+}CD44^{+}$ tumor cells are a particular population responsible for hematogenous metastasis in liver cancers and that these cells might be targets for treatment of HCC metastasis.

***Keywords*:** tumor-initiating cells; hepatocellular carcinoma; metastasis

Cell Research (2012) **22**:259-272. doi:10.1038/cr.2011.139; published online 23 August 2011

Introduction

Hepatocellular carcinoma (HCC), which accounts for 90% of primary liver cancers, is associated with a high mortality rate ($16.1/10^5$) worldwide and is the second leading cause of cancer-related deaths in China [1]. The post-surgical 5-year survival rate remains low, largely due to the high recurrence rate [2]. Intrahepatic and distant metastasis, mainly through hematogenous dissemination, is responsible for most cases of HCC relapse [3]. HCC vascular invasion, characterized by the formation of tumor thrombi in the portal or hepatic vein, is responsible for early recurrence and likely predicts poor prognosis [4, 5]. Therefore, it is urgent to understand the mechanisms of vascular invasion in liver cancers in order to develop novel treatments against HCC recurrence.

Hematogenous metastasis is an integrated and stepwise process in which tumor cells detach from the primary tumor into the stroma and invade blood vessels. This is followed by a secondary growth at a distant site [6], during which only a small group of tumor cells manage to form distant metastatic lesions. However, the exact identity of these tumor cells is largely unknown. Recent evidence suggests the existence of tumor-initiating cells (TICs), a small population of tumor cells capable of sustaining tumor formation/growth [7, 8]. These tumors could develop from an extremely small number of cells when implanted into experimental animals; the cells divide to self-renew and generate progeny to create the tumor bulk. TICs are also important for metastasis in certain solid cancers, such as breast and pancreatic cancers [9, 10]. In liver cancers, CD133, a transmembrane hematopoietic stem cell antigen [11], has been identified

*These two authors contributed equally to this work.
Correspondence: Yizheng Wang[a], Feng Shen[b]
[a]E-mail: yzwang@ion.ac.cn
[b]E-mail: shenfengdfgd@yahoo.com.cn
Received 25 January 2011; revised 20 May 2011; accepted 7 July 2011; published online 23 August 2011

as a putative marker of TICs [12, 13]. Several immunohistochemical studies in HCC specimens have revealed controversial results regarding the association of CD133 expression with metastasis occurrence [14, 15]. However, direct evidence supporting a role of $CD133^+$ cells in HCC metastasis is largely lacking. CD44, a molecule important for cell migration, is involved in the metastasis of multiple cancers, including liver cancer [16, 17]. We therefore hypothesized that $CD133^+CD44^+$ cells might be the subgroup of tumor cells that is responsible for hematogenous metastasis in liver cancer.

In this study, we reported that $CD133^+CD44^{high}$, but not $CD133^+CD44^{low/-}$, $CD133^-CD44^{high}$ or $CD133^-CD44^{low/-}$, tumor cells were responsible for intrahepatic or lung metastasis. $CD133^+CD44^+$ and $CD133^+CD44^-$ tumor cells were two populations of cells with distinct gene expression profiles. Our results suggest that targeting $CD133^+CD44^+$ tumor cells might be a new strategy for the treatment of human HCC.

Results

CD133 expression was associated with vascular invasion in liver cancers

We first examined the expression of CD133 in human HCC specimens and normal liver tissues (NTs) by immunohistochemistry (IHC; Figure 1A). As shown in Figure 1B and 1C, more $CD133^+$ cells and cells with stronger CD133 staining were found in metastatic groups (M) compared to non-metastatic (NM) and NT groups. Furthermore, we did not find a significant difference in the number of $CD133^+$ cells and their staining intensity between the primary tumors and the corresponding portal vein tumor thromboses (PVTTs), suggesting that primary tumors and the PVTT might have similar cells of origin. Collectively, these results suggest that an increased number of $CD133^+$ tumor cells is associated with vascular invasion in HCC.

$CD133^+$ tumor cells were superior in clonogenic growth but not in invasion

We next compared CD133 expression (Supplementary information, Table S1) and invasion ability in six HCC cell lines. Increased CD133 expression, as determined by transwell assay, was not associated with invasive abilities (Figure 2A). Consistently, the $CD133^+$ cells isolated from PLC8024, Hep3B and pHCC1 did not have superior invasion ability compared to $CD133^-$ cells (Figure 2B).

Further studies revealed that the $CD133^+$ cells generated 2.5- to 10-fold more colonies than did the $CD133^-$ cells did in most HCC cells tested (Figure 2C), which is consistent with the previously reported growth advantage of $CD133^+$ cells as TICs [7]. Moreover, the CD133-overexpressing cell lines and the $CD133^+$ tumor cells showed enhanced resistance to paclitaxel- or cisplatin-induced cytotoxicity (Supplementary information, Figure S2A and S2B), another important feature of TICs [7]. We then knocked down CD133 in the pHCC1, pHCC2 and Hep3B cells by specific shRNA (Figure 2D). The CD133-silenced Hep3B cells, but not pHCC1 (Figure 2E) or pHCC2 (Supplementary information, Figure S3A) cells, formed fewer colonies than control cells. However, CD133 downregulation did not change the drug resistance in the Hep3B cells (Supplementary information, Figure S2C). Collectively, these results suggest that the $CD133^+$ cells acted as TICs and were superior in cell growth, but not in cell invasion, and that CD133 might be important for the clonogenic growth of some HCC cells.

CD44 expression was associated with vascular invasion in liver cancers

We examined the expression of other surface antigens associated with tumor metastasis, including CD44, urokinase-type plasminogen activator receptor [18] and CXC chemokine receptor 4 [19] in HCC cell lines. As shown in Supplementary information, Tables S1 and S2, it was clear that CD44 expression was associated with invasiveness.

We further examined the expression of CD44 in HCC specimens and NTs (Figure 3A). As shown in Figure 3B, the number of $CD44^+$ cells in the M group was higher than that in the NM and NT groups, and CD44 staining was not different between the M and PVTT groups. In addition, some sinusoid lining cells in the normal liver and mononuclear cells in the tumor were positive for CD44. Moreover, CD44 expression was enriched at the tumor edge of metastatic HCC specimens compared with that in the tumor center (Figure 3C and Supplementary information, Figure S1B), which emphasized the importance of CD44 in metastasis. Taken together, these results suggest that an increased number of $CD44^+$ tumor cells might play a role in vascular invasion.

$CD44^{high}$ HCC cells were superior in vascular invasion but not in clonogenic growth

We then compared the invasive abilities of the $CD44^+$ ($CD44^{high}$) and $CD44^-$ ($CD44^{low/-}$) cells using the transwell assay. As shown in Figure 4A, invasion by the $CD44^+$ ($CD44^{high}$) cells was two- to six-fold higher compared to that of the $CD44^-$ ($CD44^{low/-}$) cells in most tested cell types. Because tumor cells need to transmigrate through microvessels during hematogenous metastasis, we examined whether the $CD44^+$ ($CD44^{high}$) cells pos-

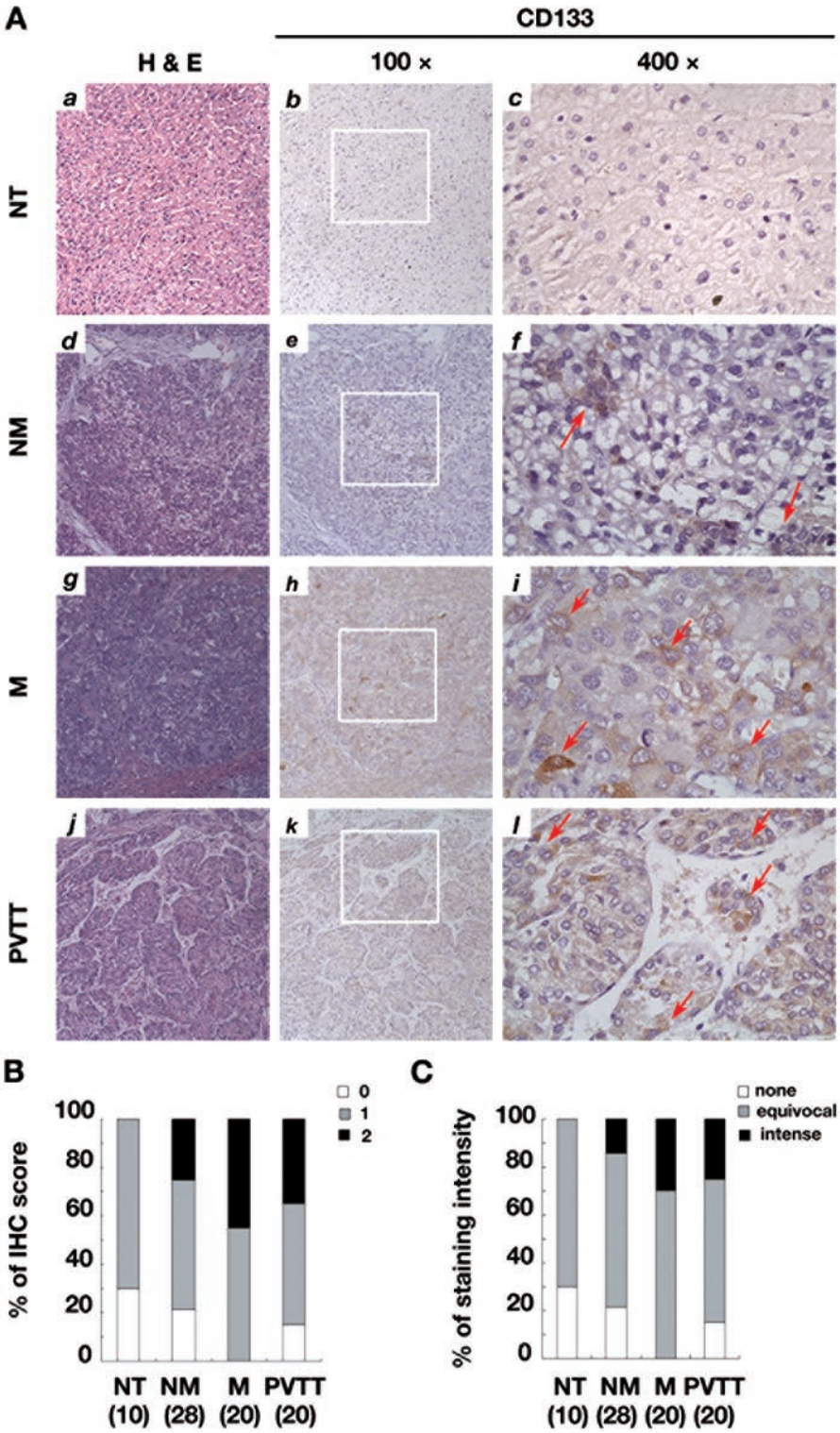

Figure 1 CD133 expression was associated with vascular invasion in liver cancers. **(A)** Representative images of H&E or CD133 staining in normal liver tissues (NTs, *a*-*c*), HCC specimens without metastasis (NM, *d*-*f*), primary tumors of metastatic HCC (M, *g*-*i*) and portal vein tumor thrombus (PVTT, *j*-*l*). Panels *c*, *f*, *i* and *l* are the enlarged images of the areas within the rectangles in *b*, *e*, *h* and *k*, respectively. Arrows in *f*, *i* and *l* indicate $CD133^+$ tumor cells. Original magnification, 100× (*a*, *b*, *d*, *e*, *g*, *h*, *j*, *k*); 400× (*c*, *f*, *i*, *l*). **(B)** Statistics regarding the CD133 IHC scores ($P = 0.037$, M vs NM; $P = 0.002$, M vs NT; and $P = 0.267$, M vs PVTT) **(C)** Statistics regarding the CD133 staining intensities ($P = 0.030$, M vs NM; $P = 0.005$, M vs NT; and $P = 0.318$, M vs PVTT).

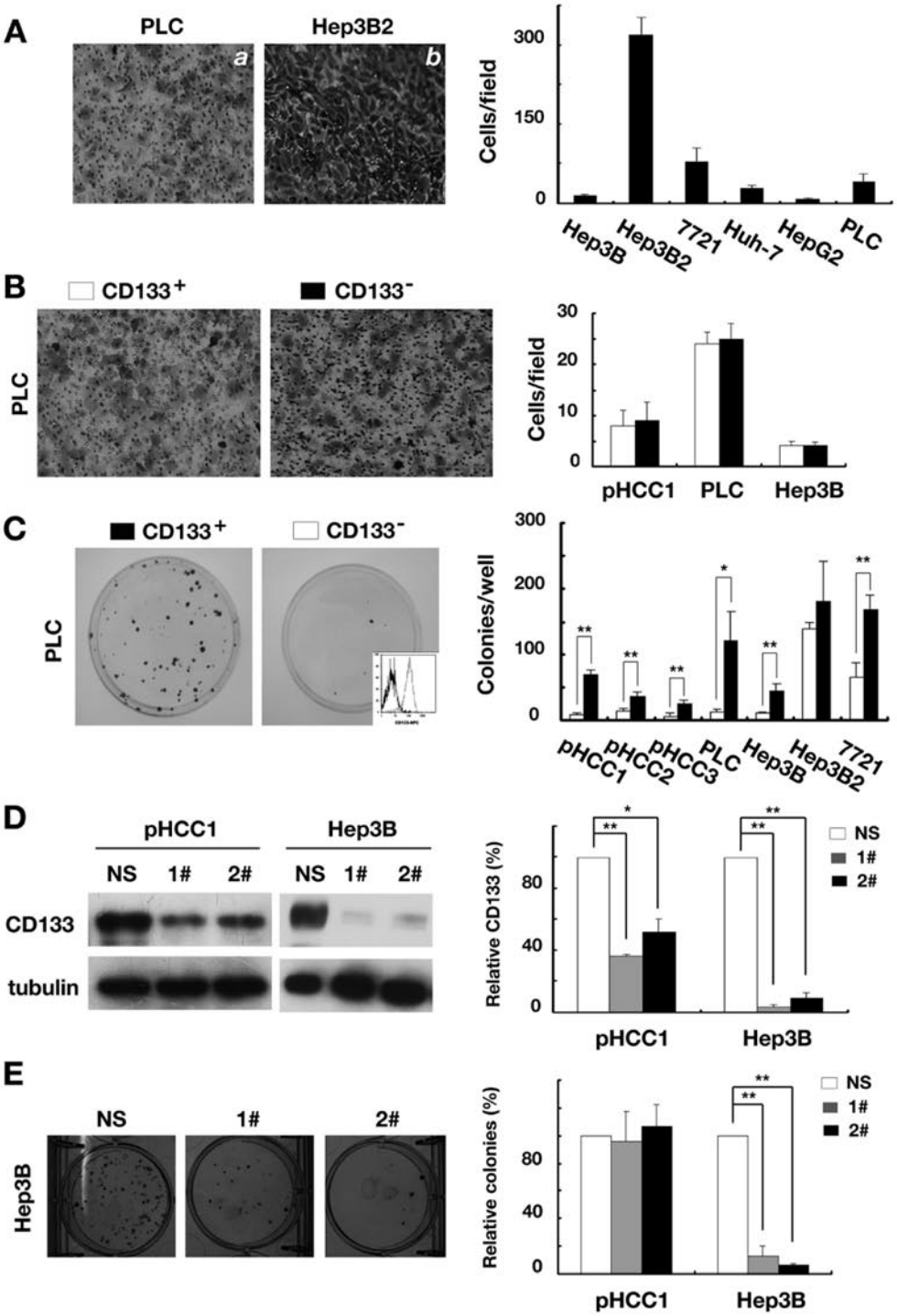

Figure 2 CD133$^+$ tumor cells were superior in clonogenic growth but not in invasion. **(A)** Representative images of invaded HCC cells in transwell assays (100×; left) and the related statistics (right). PLC, PLC8024; 7721 and SMMC-7721. **(B)** Representative images of invaded CD133$^+$ and CD133$^-$ PLC8024 cells (100×) in transwell assays (left) and the related statistics (right). **(C)** Representative images of colonies formed from sorted PLC8024 cells (left) and the related statistics (right). The flow cytometry plot shown in *a* is isolated CD133$^+$ (gray) and CD133$^-$ cells (black). **(D)** Western blotting of CD133 levels in pHCC1 and Hep3B cells infected with virus of non-sense (NS) or RNAi no. 1 and no. 2 against CD133 (left), and the statistics related to CD133 levels normalized to α-tubulin (right). **(E)** Representative images of colonies formed from infected Hep3B cells (left) and the related statistics (right). All results are expressed as mean ± SD from at least three independent experiments. *P < 0.05 and **P < 0.01.

sessed an enhanced ability of transendothelial migration. In the modeled vascular wall made by the confluent human umbilical vein endothelial cell (HUVEC) monolayer, the PLC8024 cells ($CD44^+$ cells < 10%) loosely attached and seldom moved, and were characterized by a round shape and lack of filopodia formation, even after 15 h of co-culture (Figure 4B a-e and Supplementary information, Movie S1). In contrast, the $CD44^{high}$ MHCC97H cells formed filopodia as early as 2 h after their attachment and eventually assimilated into the HUVEC layer (Figure 4B f-j) and migrated (Supplementary information, Movie S2); this was not observed for the $CD44^{low/-}$ MHCC97H cells (Figure 4B k-o and Supplementary information, Movie S3). Consistent with these observations, more $CD44^{high}$ MHCC97H and Hep3B2 cells invaded through the HUVEC-coated transwell than did their corresponding $CD44^{low/-}$ and Hep3B ($CD44^+$ cells < 1%) cells (Figure 4C). Therefore, CD44 expression levels were correlated with the invasive ability of tumor cells, especially in overcoming the vascular barrier, an important process in metastasis.

We also compared the number of colonies formed and the cell cycle profiles of the $CD44^+$ ($CD44^{high}$) and $CD44^-$ ($CD44^{low/-}$) cells and found no difference between two groups (Figure 4D and Supplementary information, Table S3). Knockdown of CD44 in the Hep3B2 and SMMC-7721 cells did not affect their growth but greatly reduced the number of invaded cells (Figure 4E and Supplementary information, Figure S3B-S3D). Taken together, these results suggest that the $CD44^{high}$ HCC cell population has a superior vascular invasion ability, but not clonogenic growth ability, and that CD44 is required for cell invasion.

$CD133^+CD44^{high}$ HCC cells were responsible for tumor metastasis

Because the $CD133^+$ and $CD44^{high}$ cells were superior in clonogenic growth and invasion, respectively, $CD133^+CD44^{high}$ HCC cells might be responsible for hematogenous metastasis of liver cancers. We examined tumor formation and metastasis using sorted $CD133^+CD44^{high}$, $CD133^+CD44^{low/-}$, $CD133^-CD44^{high}$ and $CD133^-CD44^{low/-}$ SMMC-7721 or MHCC97L cells.

In all xenografts, $CD133^+CD44^{high}$ and $CD133^+CD44^{low/-}$ sub-populations, but not $CD133^-CD44^{high}$ and $CD133^-CD44^{low/-}$, formed tumors in the liver (Figure 5A and Supplementary information, Table S4), which was consistent with the results of tumor sphere formation *in vitro* (Figure 5B). In addition, our serial dilution transplantation of different subgroups of tumor cells from human HCC specimens also indicated that the $CD133^+CD44^+$ and $CD133^+CD44^-$ cells had a high tumorigenicity in the SCID mice (Supplementary information, Figure S4 and Table S5). These results demonstrated the enhanced ability of the $CD133^+$ cells in self-renewal and tumorigenicity, further supporting CD133, but not CD44, as a marker for TICs. For SMMC-7721-implanted mice, lung metastasis was not detected. However, of seven mice injected with $CD133^+CD44^{high}$ cells, five developed tumors in the liver and four of them showed intrahepatic metastatic nodules; similar visible intrahepatic metastasis was not found in mice injected with $CD133^+CD44^{low/-}$ cells (Figure 5A and Supplementary information, Table S4). H&E staining revealed that the $CD133^+CD44^{high}$ cells demonstrated microvascular invasion and possessed more aggressive tumor edges compared to $CD133^+CD44^{low/-}$ cells (Figure 5C b-d and f-g), although both tumors displayed analogous tumor cell morphology and density (Figure 5C a and e) at the tumor center. In the MHCC97L-implanted mice, all the five mice injected with $CD133^+CD44^{high}$ cells developed tumors in the liver, and four of those developed lung metastasis. In contrast, $CD133^+CD44^{low/-}$ cells did not form lung metastasis (Figure 5D and Supplementary information, Table S4). Moreover, lentivirus-mediated RNAi targeting of CD133 and CD44 in the $CD133^+CD44^{high}$ MHCC97L cells failed to produce lung metastasis, although primary tumor formation in the liver was not affected (Supplementary information, Figure S5 and Table S6). Therefore, $CD133^+CD44^{high}$ cells are a distinct population capable of inducing metastasis at very low cell numbers and in a relatively short time.

More $CD133^+CD44^+$ tumor cells were found in metastatic than in metastasis-free HCC specimens

We next examined $CD133^+CD44^+$ tumor cells in HCC patient specimens. The hepatic and lymphatic cells were stained by the antibodies against cytokeratin-18 (CK18) and CD45, respectively. As shown in Figure 6A, more $CD45^-CD133^+CD44^+$ cells were detected in metastatic HCC specimens (0.24% ± 0.25%) than in non-metastatic HCC specimens (0.06% ± 0.11%). Immunostaining further confirmed that $CD133^+CD44^+$ tumor cells, characterized as $CK18^+CD133^+CD44^+$, were found both at the primary site and at the PVTT (Figure 6B). The number of $CD133^+CD44^+$ cells between the PVTT and the primary tumor was similar (Supplementary information, Figure S6C). Because the total number of tumor cells in the PVTT was much smaller than that in the primary tumors, it is likely that the percentage of $CD133^+CD44^+$ cells in the PVTT was higher than that in the primary site. These results provided additional evidence that these cells are indeed a subgroup of cells critical for human HCC metastasis.

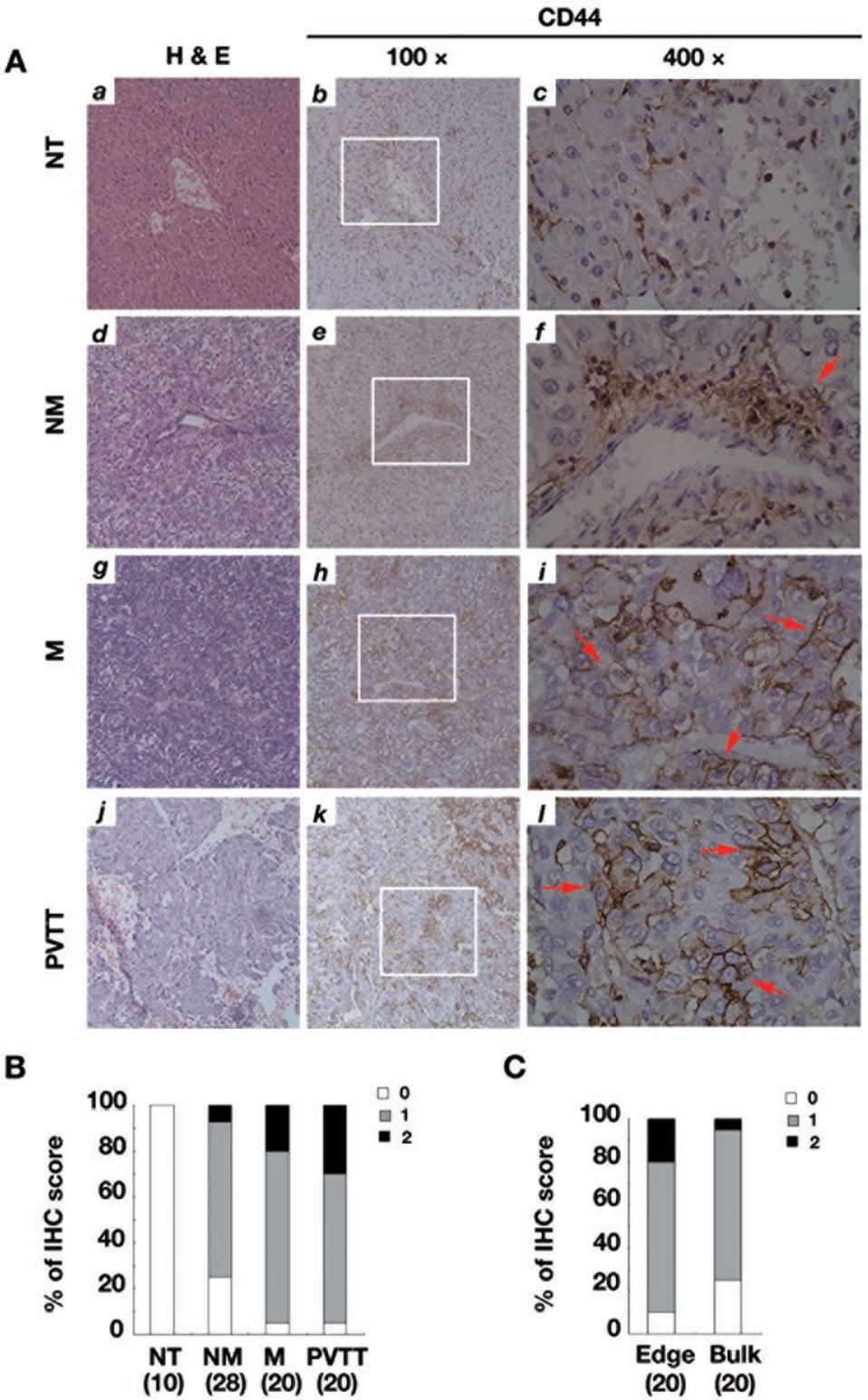

Figure 3 CD44 expression was associated with vascular invasion in liver cancers. **(A)** Representative images of H&E or CD44 staining in normal liver tissues (NTs, *a*-*c*), HCC specimens without metastasis (NM, *d*-*f*), primary tumors of metastatic HCC (M, *g*-*i*) and portal vein tumor thrombus (PVTT, *j*-*l*). Panels *c*, *f*, *i* and *l* are the enlarged images of the areas enclosed in the rectangles in *b*, *e*, *h* and *k*, respectively. Arrows in *f*, *i* and *l* indicate $CD44^+$ tumor cells. Original magnification, 100× (*a*, *b*, *d*, *e*, *g*, *h*, *j*, *k*); 400× (*c*, *f*, *i*, *l*). **(B)** Statistics related to the CD44 IHC scores (P=0.038, M vs NM; $P < 0.001$, M vs NT; and $P = 0.521$, M vs PVTT). **(C)** Statistics related to the CD44 IHC score in the tumor bulk or edge ($P = 0.037$ vs tumor edge).

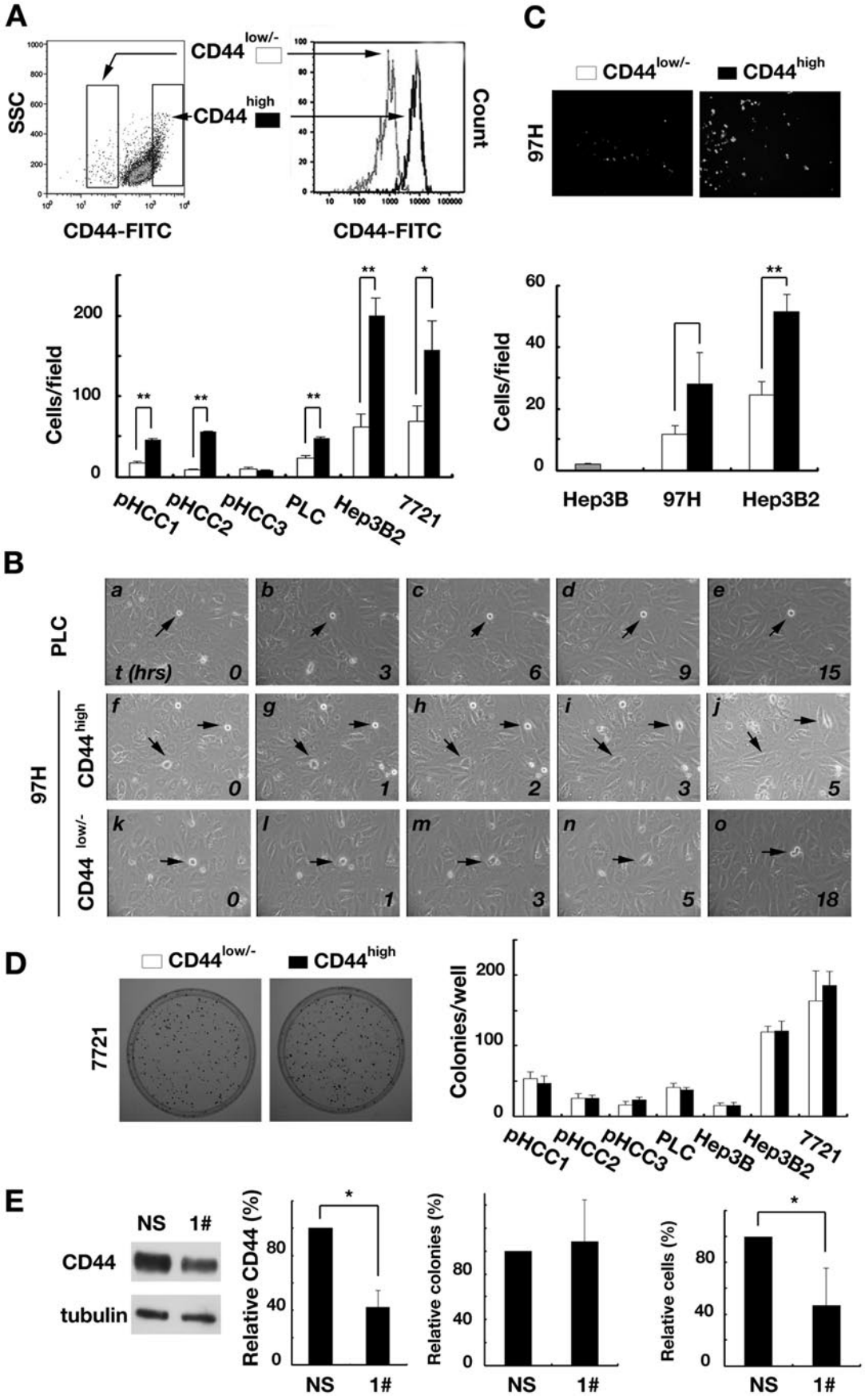
A
CD44low/-
CD44high
SSC
CD44-FITC
Count
CD44-FITC
Cells/field
pHCC1
pHCC2
pHCC3
PLC
Hep3B2
7721
C
CD44low/-
CD44high
97H
Cells/field
Hep3B
97H
Hep3B2
B
PLC
t (hrs)
97H
CD44high
CD44low/-
D
CD44low/-
CD44high
7721
Colonies/well
pHCC1
pHCC2
pHCC3
PLC
Hep3B
Hep3B2
7721
E
NS
1#
CD44
tubulin
Relative CD44 (%)
Relative colonies (%)
Relative cells (%)
NS
1#

Figure 4 $CD44^{high}$ HCC cells were superior in vascular invasion but not in clonogenic growth. **(A)** The scheme to isolate $CD44^{high}$ and $CD44^{low/-}$ HCC cells (upper left), the purity of the isolated subsets (upper right) and statistics regarding the invasiveness of sorted HCC cells (lower). PLC, PLC8024; 7721, SMMC-7721. **(B)** Representative time-lapse images of PLC8024 cells (*a*-*e*), isolated $CD44^{high}$ (*f*-*j*), $CD44^{low/-}$ (*k*-*o*) and MHCC97H (97H) cells co-cultured with HUVEC cells at the indicated times (lower right). Arrows indicate tumor cells under observation. **(C)** Representative images of transmigrated MHCC97H cells (100×) in the transendothelial migration assay (left) and related statistics (right) **(D)** Representative images of colonies formed from sorted $CD44^{high}$ and $CD44^{low/-}$ cells (left) and related statistics (right). **(E)** Western blotting of CD44 levels in Hep3B2 cells infected with virus containing non-sense (NS) or RNAi no. 1 against CD44 and statistics related to the CD44 levels normalized to α-tubulin (left). Statistics related to colony formation or cell invasion of infected Hep3B2 cells (right). All results are expressed as mean ± SD from at least three independent experiments. *$P < 0.05$ and **$P < 0.01$.

$CD133^+CD44^+$ and $CD133^+CD44^-$ cells exhibited distinct gene expression profiles

We next investigated whether the $CD133^+CD44^+$ and $CD133^+CD44^-$ cells were distinct populations. We found that genes associated with tumor metastasis, such as matrix metalloproteinases (MMP2, MMP9 and MMP12) [20] and chemokines (CXCL1, CCR5 and CCL4) [21], were upregulated in the $CD133^+CD44^+$ cells compared with the $CD133^+CD44^-$ cells (Figure 7A). Further microarray analysis of the $CD133^+CD44^+$ and $CD133^+CD44^-$ tumor cells from different HCC patients clustered them into two separate subgroups, suggesting that the $CD133^+CD44^+$ cells possessed distinct gene expression features (Figure 7B). In contrast to the $CD133^+CD44^-$ cells, 24 genes were upregulated and 52 genes were downregulated in the $CD133^+CD44^+$ cells (Supplementary information, Table S7). This included the upregulation of several metastasis-related pathways, such as CCL4, CCR5, DKK3 and MMP12 [22, 23, 24] (Figure 7C). Together, these results suggest that $CD133^+CD44^+$ and $CD133^+CD44^-$ cells display distinct gene signatures, which might result in their different abilities in inducing metastasis.

Discussion

We showed here that $CD133^+CD44^{high}$ cells play a key role in hematogenous metastasis of liver cancers, in which CD133 is responsible for tumor growth and CD44 is important for invasion, two important factors in tumor metastasis. Our results also suggest that $CD133^+$ cells act as TIC-like populations because they exhibited enhanced abilities in colony formation and tumorigenicity. This may be important for tumor cells to protect against multiple insults during metastasis. However, the $CD133^+$ tumor cells were not necessarily highly invasive [9, 15]. For example, $CD133^+CXCR4^+$ pancreatic cancer cells, but not $CD133^+CXCR4^-$ cells, invade aggressively [9]. We found that CD44, in addition to CD133, also had a critical role in tumor metastasis. In our work, CD133 and CD44 expression were associated with other pathological features besides PVTT formation (Supplementary information, Table S8), which was different from a previous report [15]. This discrepancy might be due to the difference in cohort numbers.

Recently, based on studies of HCC cell lines, $CD133^+$ and $CD44^+$ were proposed to be markers of TICs in liver cancers [25]. It was unknown whether the properties of $CD44^+$ or $CD44^-$ cells were similar to those found in HCC specimens because of a preference for CD44 expression in cell lines over HCC specimens [26]. Our results suggested that the cell lines expressing high CD44 levels were similar to the $CD44^+$ or $CD44^-$ cells from primary HCC in terms of cell growth and invasion, and that CD44 was a marker of an invasive, but not tumorigenic, sub-population. Although we noticed that the invasive ability of $CD44^{high}$ cells varied greatly between different cell lines, this difference might be caused by their distinct genetic backgrounds as well as the involvement of other genes in the regulation of cell invasion.

The $CD44^+CD90^+$ HCC cells were reported to be highly invasive [27]. Although both CD133 and CD90 were proposed as markers of liver progenitor cells [28, 29], they might represent distinct populations. First, CD90 and CD133 mark for mesenchymal and hematopoietic origin, respectively [28, 30]. Second, we (data not shown) and others [22, 23] found that $CD133^+$cells, but not $CD90^+$ cells, partially overlap with the $ALDH^{high}$ or $EpCAM^+$ TICs of HCC. As multicentric occurrence is frequently observed in HCC [24], $CD133^+$ and $CD90^+$ cells might coexist as highly tumorigenic populations, reflecting diverse tumor origin or subtypes.

Although an important finding of the current study is that knockdown of CD133 and CD44 affected tumor growth and invasion, respectively, cDNA microarray data suggested that other molecules might also be important for the enhanced metastatic potential of $CD133^+CD44^+$ tumor cells. We noticed that some molecules involved in the HCC metastatic process (twist, snail, slug and zeb) were not present in the differentially regulated genes [31, 32]. As these genes were overexpressed in a subgroup of HCC patients [31, 32], increasing the patient numbers

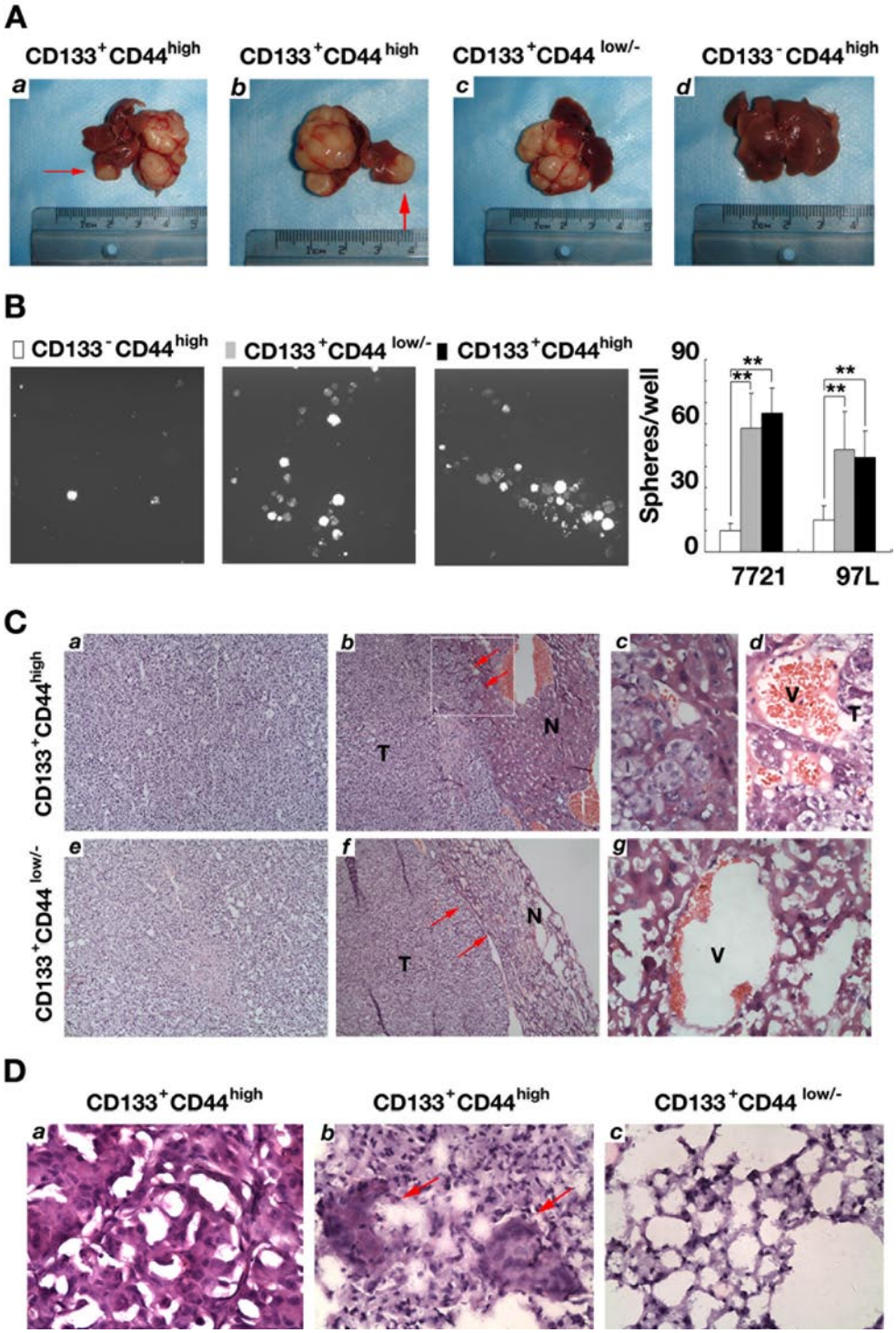

Figure 5 CD133^{+}CD44^{high} HCC cells were responsible for tumor metastasis. **(A)** Representative images of tumor formation in the liver or intrahepatic metastatic nodules as indicated in nude mice implanted with sorted SMMC-7721 cells. **(B)** Representative images of cell spheres formed by sorted SMMC-7721 (left) and the related statistics (right) 7721 (SMMC-7721), 97L (MHCC97L). **(C)** Histological analysis of the tumor center (*a*, *e*), tumor border (*b*, *f*) and microvessels (*d*, *g*) in liver tumors, formed by sorted SMMC-7721 cells. Panel *c* is the enlarged image of the area enclosed by the rectangle in *b*. Original magnification, 100× (*a*, *b*, *e*, *f*); 400× (*c*, *d*, *g*). N, normal tissue; T, tumor; V, vessel. **(D)** Representative images of H&E staining (400×) in liver tumors or lung specimens from nude mice implanted with sorted MHCC97L. Arrows indicate micrometastasis in the lung. Liver tumor tissues are shown in *a* and lung tissues in *b,c*. All results are expressed as mean ± SD from at least three independent experiments. $^{**}P < 0.01$.

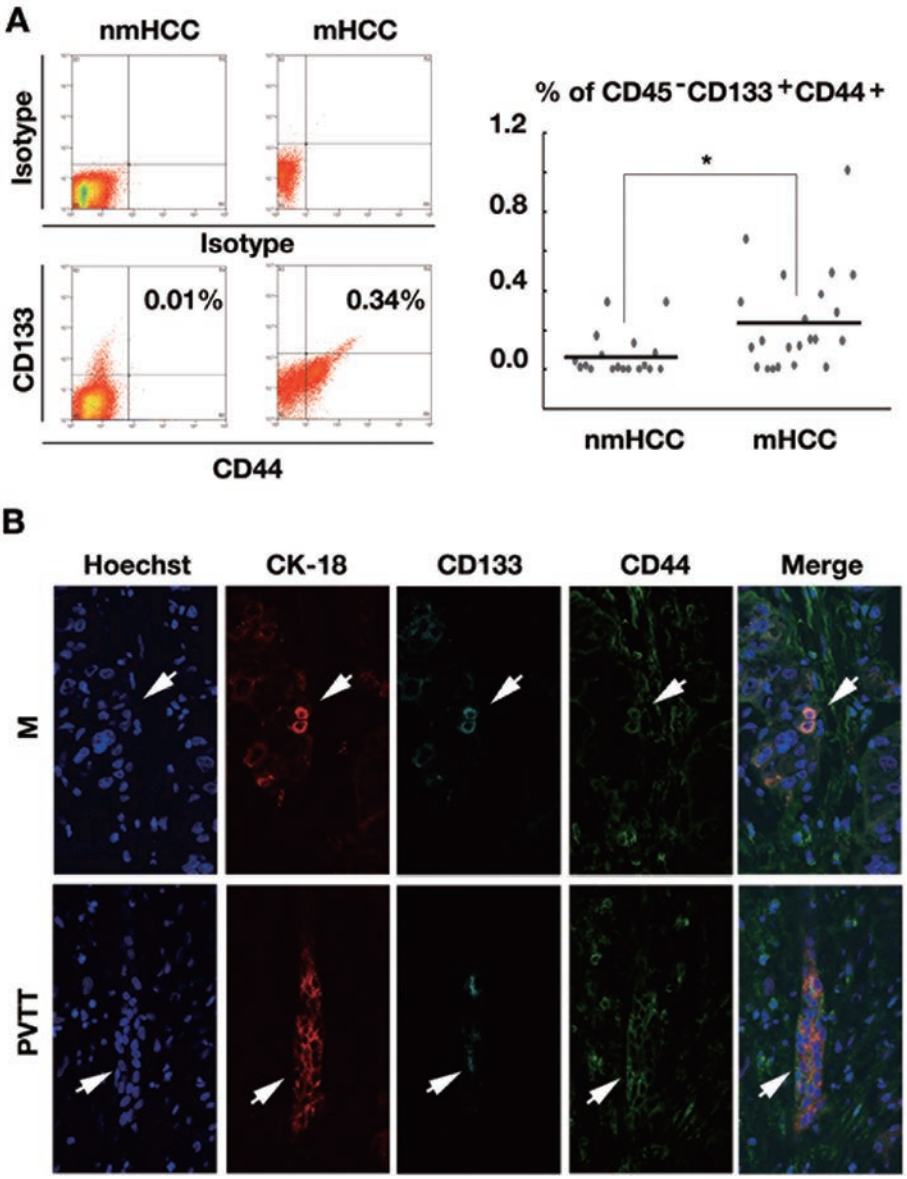

Figure 6 More $CD133^+CD44^+$ tumor cells were found in metastatic than in metastasis-free HCC specimens. **(A)** Representative flow cytometry plot of $CD45^-CD133^+CD44^+$ cells in metastatic (mHCC) or metastasis-free (nmHCC) HCC samples (left) and the related statistics (right). Images of isotype labeling are in the upper left. **(B)** Representative images of $CK18^+CD133^+CD44^+$ cells (400×), as indicated in the primary tumor (M) and portal vein tumor thrombus (PVTT). *P < 0.05.

for microarray analysis might extend the list of genes expressed differently. Therefore, CD133 and CD44 could be regarded as markers of multiple pathways through which tumor metastasis is jointly promoted. As $CD44^-$ cells might convert to $CD44^+$ cells in some conditions (Supplementary information, Table S12) [33], it is possible that tumor metastases in $CD133^+CD44^-$ xenografts might be postponed, but not prevented.

In summary, the $CD133^+CD44^+$ HCC cells were critical for HCC hematogenous metastasis. Both molecules might represent metastasis-facilitating pathways that have been integrated in these cells. The retrospective analysis of 40 HCC patients in our study has shown a close correlation between the number of $CD133^+CD44^+$ cells and tumor metastasis. Monitoring $CD133^+CD44^+$ tumor cells could be important for the prediction of HCC hematogenous metastasis. A prospective study is needed to evaluate its predictive role in the disease.

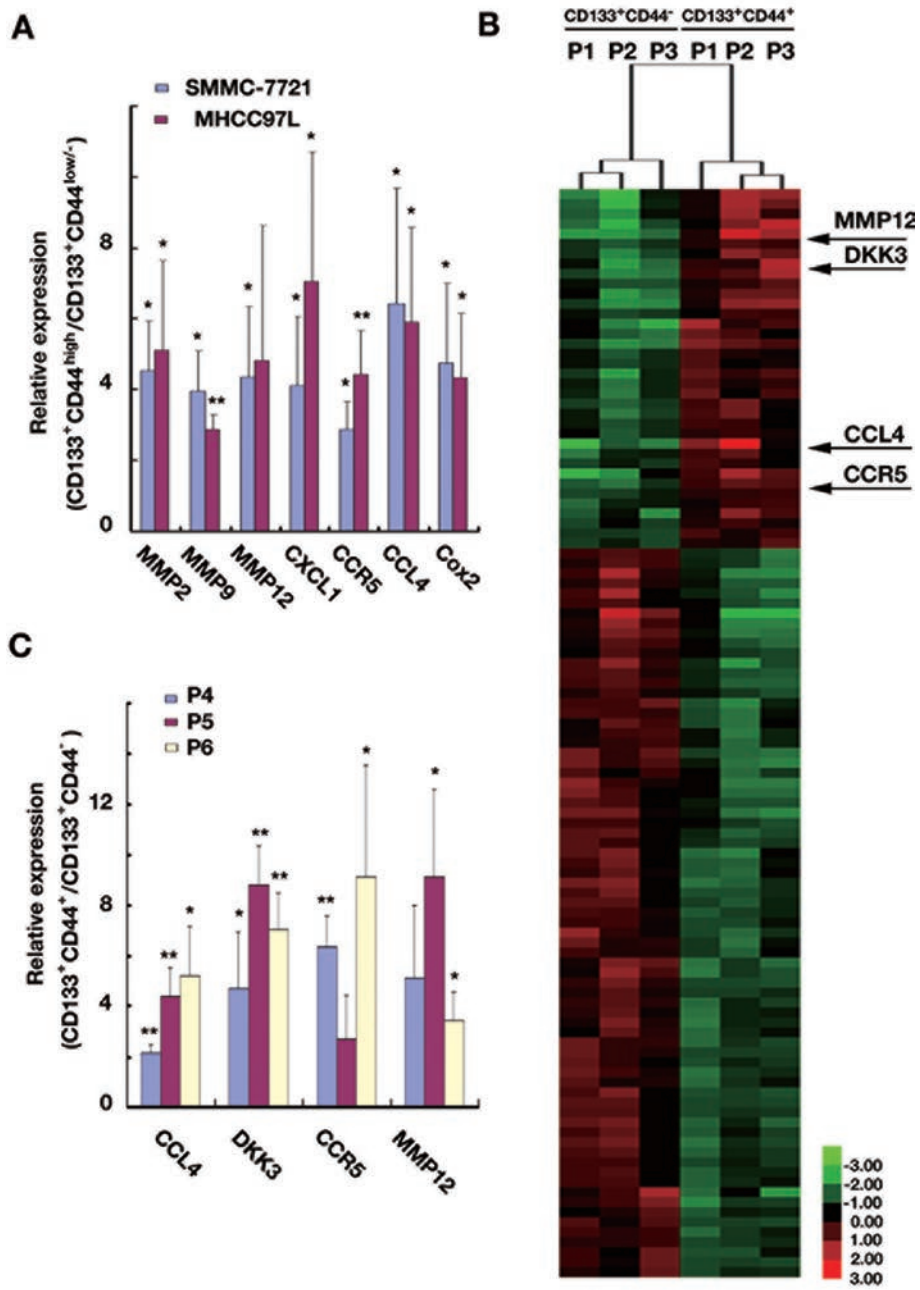

Figure 7 $CD133^+CD44^+$ and $CD133^+CD44^-$ cells were genetically different populations. **(A)** Comparison of gene expression levels between $CD133^+CD44^{high}$ and $CD133^+CD44^{low/-}$ SMMC-7721 or MHCC97L cells by real-time PCR. **(B)** The hierarchical cluster of differentially expressed probes in $CD133^+CD44^+$ and $CD133^+CD44^-$ cells based on cDNA microarray analysis. Genes indicated were used for real-time PCR validation in samples isolated from three additional HCC patients with metastasis (P4, P5 and P6). **(C)** The C^t value of the $CD133^+CD44^{low/-}$ ($CD133^+CD44^-$) subgroup was used as the calibrator. $^*P < 0.05$ or $^{**}P < 0.01$ vs the $CD133^+CD44^{low/-}$ ($CD133^+CD44^-$) subgroup.

Materials and Methods

Cell culture and materials

Human HCC cell lines, including HepG2, SMMC-7721, Hep3B, Hep3B2, Huh-7, PLC8024, MHCC97L and MHCC97H, were used in this work. Two strains of Hep3B from different sources have distinct surface antigen profiles and invasive abilities [25, 27, 34], and one strain with high expression of CD44 was named Hep3B2. Three primary HCC cells (pHCC1, pHCC2 and pHCC3) were isolated from three HCC patient xenografts in nude mice prepared as described previously [35]. The primary HCC cells were freshly prepared and further purified using flow

cytometry to exclude fibroblasts and inflammatory cells. All cell lines were maintained in Dulbecco's Modified Eagle's Medium (Gibco) with 10% fetal bovine serum (PAA Laboratories GmbH), high glucose and a penicillin-streptomycin mixture. HUVECs, purchased from ScienCell Research Laboratories, were maintained in endothelial cell medium (ScienCell Research Laboratories). All cultures were maintained at 37 °C in a humidified atmosphere of 5% CO_2 in air.

Rabbit polyclonal anti-CD133 antibody (Abcam) and mouse anti-CD44 (Neomarker) and anti-CK18 (Boster) mononclonal antibodies were used for IHC and western blot. The secondary antibody of Cy3-conjugated goat anti-mouse IgG was from Molecular Probes (Invitrogen). Mouse antibodies against CD133/2-PE (clone 293C3), CD133/1-APC (clone AC133, Miltenyi Biotec), CD44-FITC, CD44-PE-Cy5 (clone IM7, Bioscience Pharmingen, BD) and CD45-PerCP (BD) were used in flow cytometry analysis and cell sorting.

Patients and specimens

All tissue samples were obtained from consenting patients registered at the Eastern Hepatobiliary Surgery Hospital, Shanghai, between 2006 and 2009 and were approved by the Ethics Committee. Forty-eight HCC tissue samples were used for IHC. At the time of initial diagnosis, 28 patients had no major vascular invasion and were stratified into the NM group, whereas 20 patients had major vascular invasion, from which specimens of primary tumors (M) and their derived PVTTs were collected. Samples from the NM group were confirmed to be without microscopic vascular invasion. All patients underwent partial liver resections with curative intention or liver transplantation. NTs from 10 patients without liver cancer were categorized as the NT group. A total of 40 additional HCC specimens were used for flow cytometry analysis, 22 of which were associated with tumor metastasis (mHCC) and 18 of which were metastasis free (nmHCC). Five mHCC specimens were used for microarray experiments. All clinical data are summarized in Supplementary information, Table S9.

Immunostaining

IHC and immunofluorescence were performed as previously described [36]. In the IHC studies, the IHC score was defined according to the percentages of $CD133^+$ or $CD44^+$ tumor cells in the samples from 15-20 random fields at 400× magnification. As shown in Supplementary information, Figure S1A, the different grades of CD133 staining intensity were defined as follows: intense, in which the immunoreaction deposit was distinctly denser than the background and tissues that did not express the antigen; equivocal, in which the immunoreaction deposit was similar to the background and/or to tissues that did not express the antigen; and none, in which no immunoreaction deposit was found. The IHC scores were arbitrarily assigned according to the percentages of $CD133^+$ and $CD44^+$ tumor cells: 0 = none; 1 = 0.01 to 0.9%; and 2 ≥ 1% for CD133 and 0 = none; 1 = 0.01 to 5%; and 2 ≥ 5% for CD44.

We also examined CD44 expression in the tumor bulk or tumor edge in the M group. Tumor bulk was defined as areas that were 2-3mm away from distinguishable tumor borders, and tumor edge was defined as tumor areas that were 200-300 μm wide along the tumor border under the microscope.

Colony formation and tumor sphere formation

Colonies were formed as previously described [36]. For tumor sphere formation, 1×10^3 tumor cells were seeded in non-adhesive 12-well plates. Two weeks after seeding, cell spheres characterized by tight, spherical, non-adherent masses > 90 μm in diameter per well were observed, and their numbers were determined. All experiments were repeated at least three times.

Flow cytometry and cell sorting

Cells were stained by different antibodies according to the manufacturer's instructions. Flow cytometry was performed in a MoFlo XDP cell sorter (Beckman Coulter), and appropriate isotype-matched antibodies were used as controls. The purity and viability of isolated cells were routinely > 90%.

Invasion and transendothelial migration

The invasion assays were performed in the transwell insert with an 8 μm pore size (Corning) coated with Matrigel (BD) according to the manufacturer's instructions. The transendothelial migration assay was performed as reported previously [37]. Briefly, 1×10^5 HUVECs were first seeded in the upper chamber of the transwell insert. After HUVEC growth for 24 h to a confluent layer, 5×10^4 stable EGFP-transfected tumor cells were placed on the HUVEC layer. After transmigration for 24 h, the migrated cells on the bottom side of the insert were visualized, and the numbers were counted under the fluorescent microscope.

For time-lapse imaging, a total of 1×10^5 HUVECs were first plated on customized coverslips placed at the bottoms of 35 mm Petri dishes. After 24 h of HUVEC growth to a confluent layer, 1×10^4 stable EGFP-transfected tumor cells were seeded on the HUVEC layer. Unbound tumor cells were removed by a single wash after a 1-h co-culture. Tumor cells were confirmed to be GFP positive using fluorescent microscopy. The dish was then transferred to the imaging platform, which was equipped with a heat plate to maintain the temperature inside the dish at 37 °C. Mineral oil was added to the surface of the medium to avoid evaporation. The tumor cells were observed under 100× magnification using a light microscope. The image was generated by a JVC TKC1381 camera (Yokohama). One frame was taken every 6 min for 15-24 h. Images of at least five cells in each group were analyzed.

RNAi and western blot

The sequences for lentivirus-based RNAi against CD133 and CD44 are provided in Supplementary information, Table S10. Lentivirus production was achieved as previously described [38], and a multiplicity of infection of five was used to infect HCC cells. Total protein was extracted 72 h after infection and used for western blotting as described previously [35]. The density was quantified by scanning the bands.

Tumor xenograft models

Four-week old male BALB/c nude mice were maintained and cared according to the institutional guidelines. In brief, 1×10^4 sorted SMMC-7721 or MHCC97L cells were injected into the mice in the left lobes of the liver. Animals were sacrificed 3 months after implantation. Intrahepatic metastasis was defined by visible tumor nodules on the opposite liver lobe without cell injection. The absence of tumor nodules in the abdominal cavity and incision sites served as controls of a successful operation without

tumor cell leakage. The lung metastasis was diagnosed as reported previously [39] and confirmed by experienced pathologists.

Microarray analysis and real-time PCR analysis

The RNA for the microarray experiments was extracted from $CD133^+CD44^+$ and $CD133^+CD44^-$ tumor cells, sorted from the specimens of five HCC patients with metastasis, by flow cytometry. Microarray experiments were performed in the whole human genome oligo microarray (Agilent Technologies) at the National Engineering Center for Biochip at Shanghai. Quantile normalization was used to equalize the distribution of probe intensities for each array in a set of arrays, and two-sample *t*-statistics were computed for each gene. Six of ten microarrays (paired arrays for three patients) were chosen for gene expression analysis based on a CD44 probe fold change ≥ 2 in the $CD133^+CD44^+$ groups versus the paired $CD133^+CD44^-$ groups. The differentiated genes were selected based on the criteria of $P \leq 0.05$ and a fold change of ≥ 2 of their expression values between the two groups. The array clustering was performed by Cluster 3.0. The data were deposited in the GEO database (GSE26321).

For real-time PCR, cDNA was created using the SuperScript III CellsDirect cDNA Synthesis Kit (Invitrogen) according to the manufacturer's protocol. Real-time PCR was performed on the LightCycler 480 (Roche) using the LightCycler 480 SYBR Green I Master Kit according to the manufacturer's protocol. Primer sequences are provided in Supplementary information, Table S11. For each target gene, the fold change in expression levels between normal and tumor specimens was evaluated using the $2^{-\Delta\Delta Ct}$ method. Raw data were normalized using values from the 18SrRNA reference gene. For each cell line or patient, the normalized values of each biological triplicate were averaged before the calculation of the $-\Delta\Delta Ct$ using the $CD133^+CD44^-$ or the $CD133^+CD44^{low/-}$ group as a calibrator.

Statistical analysis

Results for continuous variables were expressed as mean ± SD. The Kruskal-Wallis χ^2-test was used to determine the significance of association between groups or proportions. Student's *t*-test was used to compare the means of results where appropriate. A value of $P \leq 0.05$ was considered statistically significant. All analyses were performed using SPSS 11.5 software (SPSS).

Acknowledgments

We thank Qian Hu, Weifang Jiang from the Institute of Neuroscience, CAS and Xiaoping Liu from the Institute of Biochemistry and Cell Biology, CAS for technical assistance; Yajun Guo and Lixin Wei from the Second Military Medical University for HCC cell lines; Wenzhong Tao and Wenming Cong from the Second Millitary Medical University for pathological diagnosis; and Xia Ding from our lab for comments. This work was supported by grants from the National Basic Research Program of China (2011CBA00400), the State Key Project for Research of Infectious Diseases (2008zx10002-025) and the National Natural Science Foundation of China (30711120566).

References

1 Pisani P, Parkin DM, Bray F, Ferlay J. Estimates of the worldwide mortality from 25 cancers in 1990. *Int J Cancer* 1999; **83**:18-29.
2 Jin F, Xiang YB, Gao YT. Cancer survival in Shanghai, People's Republic of China. *IARC Sci Publ* 1998; **145**:37-50.
3 Liang XH, Loncarevic IF, Tang ZY, Yu YQ, Zentgraf H, Schroder CH. Resection of hepatocellular carcinoma: oligocentric origin of recurrent and multinodular tumours. *J Gastroenterol Hepatol* 1991; **6**:77-80.
4 Tsai TJ, Chau GY, Lui WY, *et al*. Clinical significance of microscopic tumor venous invasion in patients with resectable hepatocellular carcinoma. *Surgery* 2000; **127**:603-608.
5 Hoshida Y, Villanueva A, Kobayashi M, *et al*. Gene expression in fixed tissues and outcome in hepatocellular carcinoma. *N Engl J Med* 2008; **359**:1995-2004.
6 Chambers AF, Groom AC, MacDonald IC. Dissemination and growth of cancer cells in metastatic sites. *Nat Rev Cancer* 2002; **2**:563-572.
7 Dalerba P, Cho RW, Clarke MF. Cancer stem cells: models and concepts. *Annu Rev Med* 2007; **58**:267-284.
8 Al-Hajj M, Wicha MS, Benito-Hernandez A, Morrison SJ, Clarke MF. Prospective identification of tumorigenic breast cancer cells. *Proc Natl Acad Sci USA* 2003; **100**:3983-3988.
9 Hermann PC, Huber SL, Herrler T, *et al*. Distinct populations of cancer stem cells determine tumor growth and metastatic activity in human pancreatic cancer. *Cell Stem Cell* 2007; **1**:313-323.
10 Sheridan C, Kishimoto H, Fuchs RK, *et al*. CD44+/CD24- breast cancer cells exhibit enhanced invasive properties: an early step necessary for metastasis. *Breast Cancer Res* 2006; **8**:R59.
11 Miraglia S, Godfrey W, Yin AH, *et al*. A novel five-transmembrane hematopoietic stem cell antigen: isolation, characterization, and molecular cloning. *Blood* 1997; **90**:5013-5021.
12 Ma S, Chan KW, Hu L, *et al*. Identification and characterization of tumorigenic liver cancer stem/progenitor cells. *Gastroenterology* 2007; **132**:2542-2556.
13 Yin S, Li J, Hu C, *et al*. CD133 positive hepatocellular carcinoma cells possess high capacity for tumorigenicity. *Int J Cancer* 2007; **120**:1444-1450.
14 Song W, Li H, Tao K, *et al*. Expression and clinical significance of the stem cell marker CD133 in hepatocellular carcinoma. *Int J Clin Pract* 2008; **62**:1212-1218.
15 Salnikov AV, Kusumawidjaja G, Rausch V, *et al*. Cancer stem cell marker expression in hepatocellular carcinoma and liver metastases is not sufficient as single prognostic parameter. *Cancer Lett* 2009; **275**:185-193.
16 Washington K, Telen MJ Gottfried MR. Expression of cell adhesion molecule CD44 in primary tumors of the liver: an immunohistochemical study. *Liver* 1997; **17**:17-23.
17 Mathew J, Hines JE, Obafunwa JO, Burr AW, Toole K, Burt AD. CD44 is expressed in hepatocellular carcinomas showing vascular invasion. *J Pathol* 1996; **179**:74-79.
18 Zheng Q, Tang ZY, Xue Q, *et al*. Invasion and metastasis of hepatocellular carcinoma in relation to urokinase-type plasminogen activator, its receptor and inhibitor. *J Cancer Res Clin Oncol* 2000; **126**:641-646.
19 Schimanski CC, Bahre R, Gockel I, *et al*. Dissemination of hepatocellular carcinoma is mediated via chemokine receptor CXCR4. *Br J Cancer* 2006; **95**:210-217.

20 Woo M, Park K, Nam J, Kim JC. Clinical implications of matrix metalloproteinase-1, -3, -7, -9, -12, and plasminogen activator inhibitor-1 gene polymorphisms in colorectal cancer. *J Gastroenterol Hepatol* 2007; **22**:1064-1070.
21 Erreni M, Bianchi P, Laghi L, *et al*. Expression of chemokines and chemokine receptors in human colon cancer. *Methods Enzymol* 2009; **460**:105-121.
22 Yamashita T, Ji J, Budhu A, *et al*. EpCAM-positive hepatocellular carcinoma cells are tumor-initiating cells with stem/progenitor cell features. *Gastroenterology* 2009; **136**:1012-1024.
23 Ma S, Chan KW, Lee TK, *et al*. Aldehyde dehydrogenase discriminates the CD133 liver cancer stem cell populations. *Mol Cancer Res* 2008; **6**:1146-1153.
24 Yasui M, Harada A, Nonami T, Takeuchi Y, Nakao A, Takagi H. Potentially multicentric hepatocellular carcinoma: clinicopathologic characteristics and postoperative prognosis. *World J Surg* 1997; **21**:860-864.
25 Zhu Z, Hao X, Yan M, *et al*. Cancer stem/progenitor cells are highly enriched in CD133(+)CD44(+) population in hepatocellular carcinoma. *Int J Cancer* 2010; **126**:2067-2078.
26 Haramaki M, Yano H, Fukuda K, Momosaki S, Ogasawara S, Kojiro M. Expression of CD44 in human hepatocellular carcinoma cell lines. *Hepatology* 1995; **21**:1276-1284.
27 Yang ZF, Ho DW, Ng MN, *et al*. Significance of CD90+ cancer stem cells in human liver cancer. *Cancer Cell* 2008; **13**:153-166.
28 Herrera MB, Bruno S, Buttiglieri S, *et al*. Isolation and characterization of a stem cell population from adult human liver. *Stem Cells* 2006; **24**:2840-2850.
29 Schmelzer E, Wauthier E, Reid LM. The phenotypes of pluripotent human hepatic progenitors. *Stem Cells* 2006; **24**:1852-1858.
30 Jones EA, Kinsey SE, English A, *et al*. Isolation and characterization of bone marrow multipotential mesenchymal progenitor cells. *Arthritis Rheum* 2002; **46**:3349-3360.
31 Lee TK, Poo R TP, Yuen AP, *et al*. Twist overexpression correlates with hepatocellular carcinoma metastasis through induction of epithelial-mesenchymal transition. *Clin Cancer Res* 2006, **12**:5369-5376.
32 Yang MH, Chen CL, Chau GY, *et al*. Comprehensive analysis of the independent effect of twist and snail in promoting metastasis of hepatocellular carcinoma. *Hepatology* 2009, **50**:1464-1473.
33 Patrawala L, Calhoun T, Li H, *et al*. Highly purified CD44+ prostate cancer cells from xenograft human tumors are enriched in tumorigenic and metastatic progenitor cells. *Oncogene* 2006, **25**:1696-1708.
34 Henry JC, Park JK, Jiang J, *et al*. mir-199a-3p targets CD44 and reduces proliferation of CD44 positive hepatocellular carcinoma cell lines. *Biochem Biophys Res Commun* 2010; **403**:120-125.
35 Morton CL and Houghton PJ. Establishment of human tumor xenografts in immunodeficient mice *Nat Protoc* 2007; **2**:247-250.
36 Shi Y, Ding X, He ZH, *et al*. Critical role of TRPC6 channels in G2 phase transition and the development of human esophageal cancer. *Gut* 2009; **58**:1443-1450.
37 Bazarbachi A, Abou Merhi R, Gessain A, *et al*. Human T-cell lymphotropic virus type I-infected cells extravasate through the endothelial barrier by a local angiogenesis-like mechanism. *Cancer Res* 2004; **64**:2039-2046.
38 Bender FL, Fischer M, Funk N, *et al.* High-efficiency gene transfer into cultured embryonic motoneurons using recombinant lentiviruses. *Histochem Cell Biol* 2007; **127**:439-448.
39 Tang ZY, Ye SL, Liu YK, *et al.* A decade's studies on metastasis of hepatocellular carcinoma. *J Cancer Res Clin Oncol* 2004; **130**:187-196.

(**Supplementary information** is linked to the online version of the paper on the *Cell Research* website.)